

# Influence of Cell Morphology in a Computational Model of ON and OFF Retinal Ganglion Cells

Tianruo Guo, *Student Member, IEEE*, David Tsai, *Member, IEEE*, John W. Morley, Gregg J. Suaning, *Senior Member, IEEE*, Nigel H. Lovell, *Fellow, IEEE* and Socrates Dokos, *Member, IEEE*

**Abstract**—We developed anatomically and biophysically detailed ionic models to understand how cell morphology contributes to the unique firing patterns of ON and OFF retinal ganglion cells (RGCs). With identical voltage-gated channel kinetics and distribution, cell morphology alone is sufficient to generate quantitatively distinct electrophysiological responses. Notably, recent experimental observations from ON and OFF RGCs can be closely reproduced by the variations in their cell morphologies alone. Our results suggest that RGC morphology in conjunction with biophysical properties and network connectivity are able to produce the diverse response repertoire of RGCs.

## I. INTRODUCTION

ON and OFF retinal ganglion cells (RGCs) demonstrate unique firing patterns [1, 2]. Recent experimental and modeling studies suggest that inherent biophysical properties [3-5] play an important role in these differences. Neuronal morphology was reported to play a vital role in shaping the response properties and the integration of neuronal inputs in many cell types throughout the central nervous system (CNS) [6, 7]. We hypothesize that similar phenomenon also occurs in RGCs. Thus the behaviors of these cells are a result of their biophysical properties, network connectivity, and importantly, the geometry of their neuronal processes.

To understand how morphology shapes the ON and OFF RGC responses, we developed models of these cells in the NEURON simulation environment, using an extension of the Fohlmeister and Miller (FM) (1997) formulation [8] on mice RGC morphological data. Such a computational approach allowed us to precisely control the cellular properties. Thus the effects of morphology on firing properties could be cleanly isolated. Our results suggested that in addition to their inherent biophysical properties, physical structures of RGCs can also largely influence their firing patterns.

T. Guo, D. Tsai, G. J. Suaning, N. H. Lovell and S. Dokos are with the Graduate School of Biomedical Engineering, University of New South Wales, Sydney, 2052, Australia. D. Tsai is also with Howard Hughes Medical Institute, Biological Sciences, Columbia University, New York, NY, USA and Bioelectronic Systems Lab, Electrical Engineering, Columbia University, New York, NY, USA. J. W. Morley is with School of Medicine, University of Western Sydney, Australia.

E-mail for correspondence: s.dokos@unsw.edu.au

## II. METHODOLOGY

### A. Cell Morphology Reconstruction

Realistic three-dimensional (3D) reconstructions of two mice RGCs were traced. One ON cell with 196  $\mu\text{m}$  average dendritic diameter and stratified at a depth of 40% in the inner plexiform layer, one OFF cell with 191  $\mu\text{m}$  average dendritic diameter, at a depth of 70% in the inner plexiform layer were filled with neurobiotin and digitally reconstructed using a confocal microscope with a 20 $\times$ 0.7 NA air and a 40 $\times$ 1.1 NA oil immersion objective lens, in conjunction with Imaris (Bitplane AG) and Fiji (National Institute of Health, USA). Morphological data were digitized in SWC format and imported into NEURON 7.2 [9]. We included in the model representations of soma, axon initial segment (AIS), axon hillock, axon and dendrites. Morphological segments were chosen to ensure the accurate spatial granularity.

### B. RGC Model

The 3D RGC model used in this study is characterized by,

$$\sigma \frac{\partial^2 V_m}{\partial x^2} = A \cdot (C_m \frac{\partial V_m}{\partial t} + J_{ion} - J_{stim}) \quad (1)$$

where  $V_m$  (mV) represents membrane potential,  $x$  is the distance along the cable,  $\sigma$  ( $\mu\text{S}\cdot\text{cm}^{-1}$ ) is the intracellular conductivity,  $A$  ( $\text{cm}^{-1}$ ) is the cell membrane area in averaged cell volume.  $J_{ion}$  ( $\mu\text{A}\cdot\text{cm}^{-2}$ ) represent the ionic currents, including seven time-dependent currents (fast sodium current, delayed-rectifying potassium current, A-type potassium current, L-type calcium current, calcium-activated potassium current, hyperpolarization-activated current, low-voltage  $\text{Ca}^{2+}$  current) and one leakage current.  $J_{stim}$  is the intracellular stimuli. In this model, the membrane capacitance ( $C_m$ ) was set to 1  $\mu\text{F}\cdot\text{cm}^{-1}$ . Intracellular axial resistance was set to 110  $\Omega\cdot\text{cm}$ . Model parameters were optimized to ensure reasonable RGC behaviors in responses to multiple stimuli. The ionic channel distributions were set as neuronal compartment-specific to reflect the proportion of ion channels in specific regions of the RGC. Since we focus on studying the isolated contribution from RGC morphologies in this study, ON and OFF RGC models shared the identical biophysical-defining model parameters and differed only in their physical structure. Details of the RGC model formulation including ionic channel kinetics and distribution can be found in the accompanying paper by Guo et al. [10].

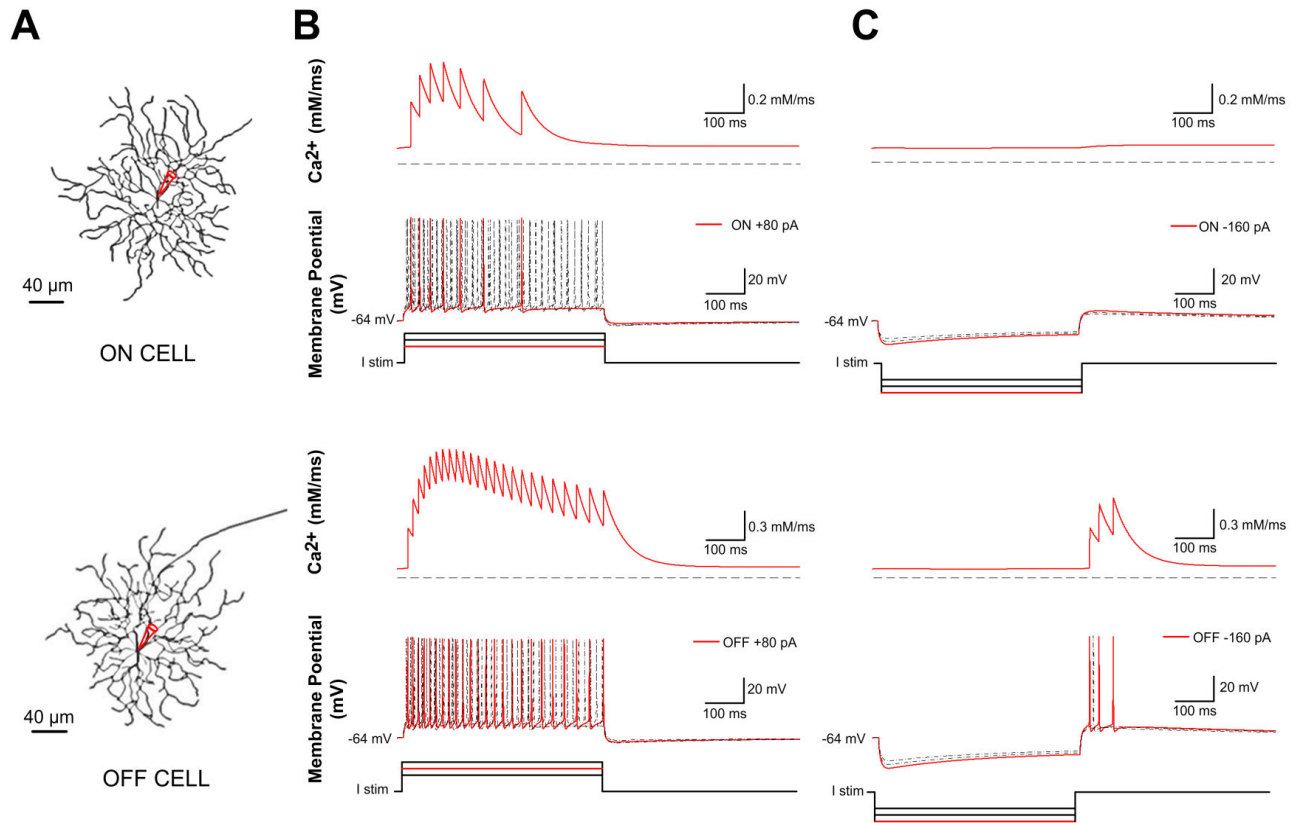


Fig. 1. A. Computer-reconstructed geometry. B and C. Multiple model-generated membrane potentials and calcium concentration while injecting a family of current pulses at the soma. The model reproduced both normal (B) and rebound (C) RGC spikes. The somatically injected depolarizing currents were of 500 ms duration with amplitudes 80, 100 and 120 pA for the ON cell and 60, 80 and 100 pA for the OFF cell. The hyperpolarizing current steps were -120, -140 and -160 pA. Red traces highlight an individual response with its corresponding stimulus trace denoted by the red step below.

All simulations were performed and analyzed in NEURON and Matlab (Mathworks).

### III. RESULTS

#### A. Morphologically-specific Responses of ON and OFF RGCs

To isolate the contribution of morphology to cellular responses, we used identical biophysics and distribution in the ON and OFF cells. Voltage responses from two RGC models were recorded during multiple depolarizing (80, 100 and 120 pA for ON cell; 60, 80 and 100 pA for OFF cell) and hyperpolarizing (-120, -140 and -160 pA) somatic current injections.

Fig. 1 illustrates the unique responses in the two RGC types due to their different morphology. The OFF cell demonstrated excitation in response to hyperpolarizing stimuli, including a slow depolarizing “sag” on hyperpolarization below resting membrane potential, and a significant rebound burst fired at termination of the hyperpolarizing step. Notably, the ON cell only showed a small passive response under the same condition. In addition,

these two cell types exhibited different spiking frequency, response latency and  $\text{Ca}^{2+}$  dynamics in response to the same levels of stimuli (as highlighted in the red traces). Finally, we also note that simulated responses reasonably matched recent experimental observations from ON and OFF RGCs [4].

#### B. Influence of Dendritic Bifurcations on Action Potential Propagation

In another simulation, we examined influence of physical dendritic structure on the action potential (AP) propagation along the dendrites. We physically disconnected the corresponding daughter branches from the primary dendrite in the computer-reconstructed RGC geometry (see Fig. 2A1-A2), and then calculated APs at each position along the dendrite in response to a somatic depolarization step (100 pA amplitude, 500 ms duration). Fig. 2 shows the effects of removing daughter branches from the primary dendrite. In both situations, in response to somatic current injection, trains of APs initiate in the soma of the RGC and propagate out into the distal dendrite (Fig. 2C1-C2 upper panel). However, branch removal resulted in considerable alterations of AP characteristics:

1. AP waveform geometry: Rate of AP change (phase plot) was used to analyze characteristics of AP waveforms [11, 12].

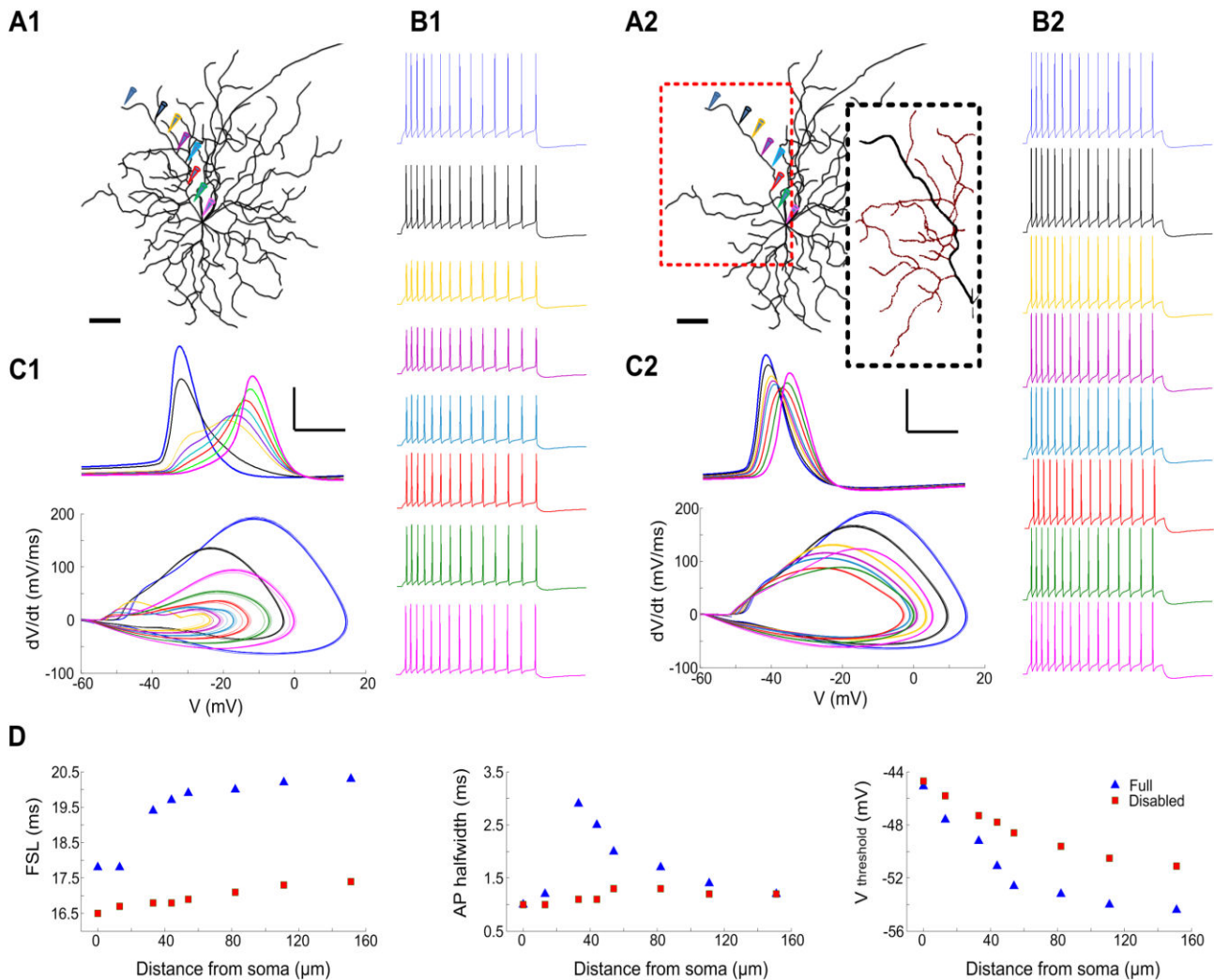


Fig. 2. Influence of dendritic branches on AP propagation. A1-A2. Reconstructed OFF RGC morphology containing an intact dendritic arbor (control, A1) or with surrounding daughter branches removed (A2) from the primary dendrite. A2 Inset: pruned branches are labelled in red. Scale bar:  $40\mu\text{m}$ . B1-B2. AP recorded in soma and dendrite. Colored traces correspond to colored electrode in A1 and A2. C1-C2. Upper. Plot of the first action potential in a spike train. Scale bar: 20 mV and 2 ms. Lower. Phase plot of  $dV/dt$  versus membrane potential ( $V$ ) for somatic and dendritic spikes. D. Comparison of model behaviors before ( $\blacktriangle$ ) and after ( $\blacksquare$ ) daughter branches were pruned. Left. First spike latency of AP in the dendrite as a function of distance. Middle. Dendritic AP duration (the width of the AP at half-amplitude) as a function of distance. Right. Dendritic spike threshold (the membrane potential at which  $dV/dt$  of spike crossed 5-20 mV/ms) as a function of distance. In both cases, spike thresholds revealed exponential decrease along the dendrite.

‘Full model’ and ‘pruned model’ indicated a clear difference in AP shape (Fig. 2C1-C2, lower panel). After peripheral branches were removed, dendritic AP waveform changed (i.e. AP peak value, AP duration, rise and fall time) during propagation were largely eliminated (also see middle panel, Fig. 2D).

2. Timing of AP occurrence: First spike latency (FSL), defined as the time difference between the stimulation termination and half-maximum amplitude of the first dendritic AP, was used to calculate AP occurrence time in the dendrites (see left panel, Fig. 2D). As shown in the FSL curve, the stronger propagation speed in the ‘bare’ dendritic tree ensures nearly simultaneous AP occurrence from soma to distal dendrites, within less than 1 ms (AP duration is 1-2 ms). In contrast, the model with a full dendritic tree experienced  $\sim 3$  ms latency between somatic and distal dendritic APs.

3. AP onset properties: The spike threshold, defined as the membrane potential at which  $dV/dt$  of the AP spike crossed 5-20 mV/ms, is an important parameter for analyzing the location of AP initiation [13, 14]. Fig. 2D (right panel) revealed that the exponential decrease of threshold voltage along the dendrite was weakened by removing the surrounding daughter branches.

#### IV. DISCUSSION AND CONCLUSION

Our simulations suggested that ON and OFF RGCs are able to reproduce biological responses by their morphological variations. In our models, all biophysical parameters describing voltage-gated channel kinetics and the ionic distribution shared the same values. Thus the individual

responses of ON and OFF cells were solely dependent on cell morphology.

The dramatic change of AP characteristics during dendritic propagation could be attributed to the current loading with a large number of bifurcation points of RGC dendrites. At a proximal branching point the orthodromic AP from the soma was distributed among multiple daughter branches, which could weaken the propagating AP by splitting the current from the primary dendrite. As the AP propagated towards the distal branches, there were progressively less branching points, and eventually a sealed end. In this condition, the AP size might increase as a result. Removing dendritic branches in the model resulted in less AP characteristic alterations and promoted a stronger AP propagation. Recent modeling studies of CA1 pyramidal neuron also suggested that removal of dendritic branches could convert a weak propagating neuron to a strong propagating neuron [15]. Interestingly, the somatic and dendritic AP waveforms simulated in the pruned model closely agree with the published dendritic AP recordings in rabbit RGCs [16], which only exhibit minimal branching points.

While we have focused on the contribution of cell morphology in this study, it should be noted that the unique electrophysiology of ON and OFF cells are also due to their inherent biophysical properties. For example, the absence and presence of rebound excitations in ON and OFF RGCs could be a result of their differently distributed ionic channels across their plasma membrane [1]. In addition, the slowing and broadening in kinetics of the dendritic AP in our simulation (Fig. 2) is consistent with lower densities of sodium and potassium current in dendrites. Strong AP propagation in the dendritic tree was impossible without active dendritic processes in our model (results not shown). The critical roles of active dendrites and corresponding ionic channel distribution in shaping RGC firing patterns are discussed in an accompanying paper [17].

Morphology was rarely examined quantitatively in the previous studies of RGC response properties (except some modeling studies [12, 18, 19]). This is probably due to the difficulty of isolating the morphology's contribution in biological experiments. However, computational studies provide a promising platform for understanding how the physical characteristics of RGCs influence their behaviors. This study was undertaken to establish a basis for realistic RGC modeling. In future studies, we intend to expand to other RGC types (~22 types of mammalian RGCs have been identified thus far), as well as incorporate physiologically relevant experimental design for further model building or validation.

#### ACKNOWLEDGMENT

This research was supported by the Australia Research Council (ARC) through a Special Research Initiative (SRI) in

Bionic Vision Science and technology grant to Bionic Vision Australia (BVA).

#### REFERENCES

- [1] D. J. Margolis and P. B. Detwiler, "Different mechanisms generate maintained activity in ON and OFF retinal ganglion cells," *J Neurosci*, vol. 27, pp. 5994-6005, 2007.
- [2] P. H. Schiller, J. H. Sandell, and J. H. Maunsell, "Functions of the ON and OFF channels of the visual system," *Nature*, vol. 322, pp. 824-825, 1986.
- [3] B. J. O'Brien, T. Isayama, R. Richardson, and D. M. Berson, "Intrinsic physiological properties of cat retinal ganglion cells," *J Physiol*, vol. 538, pp. 787-802, 2002.
- [4] D. J. Margolis, A. J. Gartland, T. Euler, and P. B. Detwiler, "Dendritic calcium signaling in ON and OFF mouse retinal ganglion cells," *J Neurosci*, vol. 30, pp. 7127-7138, 2010.
- [5] T. Kameneva, H. Meffin, and A. N. Burkitt, "Modelling intrinsic electrophysiological properties of ON and OFF retinal ganglion cells," *J Comput Neurosci*, vol. 31, pp. 547-561, 2011.
- [6] P. Vetter, A. Roth, and M. Hausser, "Propagation of action potentials in dendrites depends on dendritic morphology," *J Neurophysiol*, vol. 85, pp. 926-937, 2001.
- [7] N. Spruston, "Pyramidal neurons: dendritic structure and synaptic integration," *Nat Rev Neurosci*, vol. 9, pp. 206-221, 2008.
- [8] J. F. Fohlmeister and R. F. Miller, "Impulse encoding mechanisms of ganglion cells in the tiger salamander retina," *J Neurophysiol*, vol. 78, pp. 1935-1947, 1997.
- [9] M. L. Hines and N. T. Carnevale, "The NEURON simulation environment," *Neural Computation*, vol. 9, pp. 1179-1209, 1997.
- [10] T. Guo, D. Tsai, J. W. Morley, G. J. Suaning, N. H. Lovell, and S. Dokos, "Cell-specific modeling of retinal ganglion cell electrical activity," in *Engineering in Medicine and Biology Society (EMBC), 2013 Annual International Conference of the IEEE*, accepted.
- [11] E. M. Izhikevich, *Dynamical Systems in Neuroscience: The Geometry of Excitability and Bursting*. London, England: The MIT Press, 2007.
- [12] J. F. Fohlmeister and R. F. Miller, "Mechanisms by which cell geometry controls repetitive firing in retinal ganglion cells," *J Neurophysiol*, vol. 78, pp. 1948-1964, 1997.
- [13] Y. Yu, Y. Shu, and D. A. McCormick, "Cortical action potential backpropagation explains spike threshold variability and rapid-onset kinetics," *J Neurosci*, vol. 28, pp. 7260-7272, 2008.
- [14] B. Naundorf, F. Wolf, and M. Volgushev, "Unique features of action potential initiation in cortical neurons," *Nature*, vol. 440, pp. 1060-1063, 2006.
- [15] N. L. Golding, W. L. Kath, and N. Spruston, "Dichotomy of action-potential backpropagation in CA1 pyramidal neuron dendrites," *J Neurophysiol*, vol. 86, pp. 2998-3010, 2001.
- [16] T. J. Velte and R. H. Masland, "Action potentials in the dendrites of retinal ganglion cells," *J Neurophysiol*, vol. 81, pp. 1412-1417, 1999.
- [17] T. Guo, D. Tsai, S. Sovilj, J. W. Morley, G. J. Suaning, N. H. Lovell, and S. Dokos, "Influence of active dendrites on firing patterns in a retinal ganglion cell model," in *Engineering in Medicine and Biology Society (EMBC), 2013 Annual International Conference of the IEEE*, accepted.
- [18] J. F. Fohlmeister, E. D. Cohen, and E. A. Newman, "Mechanisms and distribution of ion channels in retinal ganglion cells: using temperature as an independent variable," *J Neurophysiol*, vol. 103, pp. 1357-1374, 2010.
- [19] D. Tsai, S. Chen, D. A. Protti, J. W. Morley, G. J. Suaning, and N. H. Lovell, "Responses of retinal ganglion cells to extracellular electrical stimulation, from single cell to population: model-based analysis," *PLoS One*, vol. 7, p. e53357, 2012.